RESEARCH ARTICLE

National Science Review
8: nwaa169, 2021
doi: 10.1093/nsr/nwaa169
Advance access publication 24 July 2020

PHYSICS

New types of topological superconductors under local magnetic symmetries

Jinyu Zou [1], Qing Xie[1], Zhida Song[2] and Gang Xu[1,*]

ABSTRACT

We classify gapped topological superconducting (TSC) phases of one-dimensional quantum wires with local magnetic symmetries, in which the time-reversal symmetry $\mathcal{T}$ is broken, but its combinations with certain crystalline symmetries, such as $M_x\mathcal{T}$, $C_{2z}\mathcal{T}$, $C_{4z}\mathcal{T}$ and $C_{6z}\mathcal{T}$, are preserved. Our results demonstrate that an equivalent BDI class TSC can be realized in the $M_x\mathcal{T}$ or $C_{2z}\mathcal{T}$ superconducting wire, which is characterized by a chiral Z^c invariant. More interestingly, we also find two types of totally new TSC phases in the $C_{4z}\mathcal{T}$ and $C_{6z}\mathcal{T}$ superinducting wires, which are beyond the known AZ class, and are characterized by a helical Z^h invariant and $Z^h\oplus Z^c$ invariants, respectively. In the Z^h TSC phase, Z pairs of Majorana zero modes (MZMs) are protected at each end. In the $C_{6z}\mathcal{T}$ case, the MZMs can be either chiral or helical, and even helical-chiral coexisting. The minimal models preserving $C_{4z}\mathcal{T}$ or $C_{6z}\mathcal{T}$ symmetry are presented to illustrate their novel TSC properties and MZMs.

Keywords: topological superconductor, magnetic symmetry, Majorana zero mode, superconducting wire

INTRODUCTION

Topological superconductors (TSCs) are new kinds of topological quantum states, which are fully superconducting gapped in the bulk but support gapless excitations called Majorana zero modes (MZMs) at the boundaries [1–5]. As analogues of the famous Majorana fermions [6], MZMs are their own antiparticles, and are proposed as the qubits of topological quantum computation because of their nonlocal correlation and non-Abelian statistic nature [7–10]. Hence, searching for TSC materials with MZMs is now an important topic in condensed matter physics, and a series of schemes have been proposed in the last decade, including the proximity effect on the surface of topological insulators [11–16] and the recently predicted intrinsic superconducting topological materials [17–25].

To identify whether a superconductor is topologically nontrivial, we should first ascertain to what topological classification it belongs. The topological classification can be highly enriched by symmetries, including time-reversal symmetry $\mathcal{T}$, particle-hole symmetry $\mathcal{P}$ and especially the crystalline symmetries [26–35]. The topology for noninteracting Hamiltonians of the 10 Altland–Zirnbauer (AZ) classes with or without $\mathcal{T}$ and $\mathcal{P}$ has been well classified [26,27]. Particularly, the Bogoliubov–de Gennes (BdG) Hamiltonians of the one-dimensional (1D) superconductors, with $\mathcal{T}$ breaking or preserving, belong to the D and DIII classes, respectively. In both cases we only have the Z_2 classification. In addition to these local symmetries, crystalline symmetries are considered for each AZ class to generalize the topological classification [28–31], and the topological crystalline superconductors protected by mirror reflection symmetry [32,33] or rotational symmetries [34,35] have been proposed. Furthermore, the TSC phase protected by the magnetic symmetries $M_x\mathcal{T}$ and $C_{2z}\mathcal{T}$ has been discussed in [34,36–38]. Nevertheless, the topological classification of superconductors with general magnetic symmetries is still an open question, and the corresponding theoretical analysis is necessary for understanding and searching for new magnetic TSC materials and MZMs.

In this paper, we focus on the topological phases of gapped superconducting wires with local magnetic symmetries (LMSs), in which $\mathcal{T}$ is broken, but its combinations with certain crystalline

[1]Wuhan National High Magnetic Field Center & School of Physics, Huazhong University of Science and Technology, Wuhan 430074, China and [2]Department of Physics, Princeton University, Princeton, NJ 08544, USA

*Corresponding author. E-mail: gangxu@hust.edu.cn

Received 10 January 2020; **Revised** 16 June 2020; **Accepted** 16 June 2020

Table 1. The topological classification of the 1D gapped superconducting systems with the LMSs $M_x\mathcal{T}$, $C_{2z}\mathcal{T}$, $C_{4z}\mathcal{T}$ and $C_{6z}\mathcal{T}$, respectively. 2×AIII form a helical Z^h classification.

$\mathcal{T}'$	$M_x\mathcal{T}$ $(n=2)$	$C_{2z}\mathcal{T}$ $(n=2)$	$C_{4z}\mathcal{T}$ $(n=4)$	$C_{6z}\mathcal{T}$ $(n=6)$
$\mathcal{T}'^n$	1	1	−1	1
$\mathcal{P}^2$	1	1	1	1
$\mathcal{S}^n$	1	1	−1	1
Invariant	Z^c (BDI)	Z^c (BDI)	Z^h (2×AIII)	$Z^h\oplus Z^c$ (2×AIII ⊕ BDI)

symmetries—those leaving each site invariant, including $M_x\mathcal{T}$, $C_{2z}\mathcal{T}$, $C_{4z}\mathcal{T}$ and $C_{6z}\mathcal{T}$—are preserved. Our analysis shows that, with $M_x\mathcal{T}$ or $C_{2z}\mathcal{T}$ symmetry, an effective BDI class TSC can be realized, which is characterized by a chiral Z^c topological invariant and protects an integer number of MZMs at each end. Remarkably, two totally new TSC phases are discussed in the superconducting wire with $C_{4z}\mathcal{T}$ or $C_{6z}\mathcal{T}$ symmetry. In the $C_{4z}\mathcal{T}$ case, the BdG Hamiltonian is characterized by a helical Z^h invariant, which can protect Z pairs of MZMs at each end. The BdG Hamiltonian with $C_{6z}\mathcal{T}$ symmetry possesses $Z^h\oplus Z^c$ invariants, which means that the helical and chiral MZMs can coexist in a single wire system. The minimal models with the LMSs $C_{4z}\mathcal{T}$ and $C_{6z}\mathcal{T}$ are presented separately, in which the TSC with helical MZMs and the TSC with helical-chiral coexisting MZMs are discussed. Our results may facilitate the ongoing search for novel TSCs.

TOPOLOGICAL CLASSIFICATION OF GAPPED SUPERCONDUCTING WIRE

We first introduce the LMSs for a magnetic superconducting wire along the z direction. Among the 1D space groups (the so-called rod group) [39], the local symmetry operators include the mirror reflection M_x and the n-fold rotation C_{nz} with $n = 2, 3, 4, 6$. Combined with $\mathcal{T}$, we obtain four types of LMSs, $\mathcal{T}' = M_x\mathcal{T}, C_{2z}\mathcal{T}, C_{4z}\mathcal{T}$ and $C_{6z}\mathcal{T}$, as tabulated in Table 1. We consider a 1D BdG Hamiltonian preserving $\mathcal{T}'$. Note that the operation of $\mathcal{T}'$ does not change the positions of electrons. Hence, it acts on the BdG Hamiltonian like a time-reversal operator

$$\mathcal{T}'H_{\rm BdG}(k)\mathcal{T}'^{-1} = H_{\rm BdG}(-k). \tag{1}$$

Here, LMS $\mathcal{T}'$ takes the form $\mathcal{T}' = U\mathcal{K}$ with $\mathcal{K}$ being the complex conjugate operator and U being a unitary matrix determined by the spatial operation and spin flipping. We employ the convention that $[\mathcal{T}, \mathcal{P}] = 0$ and set $\mathcal{P} = \tau_x\mathcal{K}$, where the Pauli matrix τ_x acts on the particle-hole degree of freedom. Combining $\mathcal{T}'$ and $\mathcal{P}$ leads to a chiral symmetry $\mathcal{S} = \mathcal{T}'\mathcal{P}$. Both $\mathcal{P}$ and $\mathcal{S}$ act on the BdG Hamiltonian as

$$\mathcal{P}H_{\rm BdG}(k)\mathcal{P}^{-1} = -H_{\rm BdG}(-k), \tag{2}$$

$$\mathcal{S}H_{\rm BdG}(k)\mathcal{S}^{-1} = -H_{\rm BdG}(k). \tag{3}$$

The chiral symmetry $\mathcal{S}$ has a series of eigenvalue pairs $\pm s_1$, $\pm s_2$, … and it can take a block-diagonal form as $\mathcal{S} = \mathrm{diag}[\mathcal{S}_{\pm s_1}, \mathcal{S}_{\pm s_2}, \ldots]$, where the subscript $\pm s_1$ denotes the direct sum of eigenvector spaces $|s_1\rangle$ and $|-s_1\rangle$. The anticommute relation (3) means that $H_{\rm BdG}(k)$ can be block diagonalized according to the eigenvalues of $\mathcal{S}^2$. In other words, $H_{\rm BdG}(k)$ can adopt the form $H_{\rm BdG}(k) = \mathrm{diag}[H_{s_1^2}, H_{s_2^2}, \ldots]$. Hence, the topological classification of the whole Hamiltonian is decomposed into examining the topology of each block and their compatibility. For each block Hamiltonian H_{s^2}, its topology is equivalent to either the BDI or the AIII class, depending on the chiral symmetry eigenvalue s. To be specific, when s is a real number, H_{s^2} is invariant under $\mathcal{T}'$ or $\mathcal{P}$, which means that it belongs to the BDI class and possesses a Z invariant expressed as $v = N_s - N_{-s}$, where the $N_{\pm s}$ are the numbers of MZMs with chiral symmetry eigenvalue $\pm s$, respectively. Additionally, when s is a complex number, H_{s^2} is transformed into $H_{s^{*2}}$ under $\mathcal{T}'$ or $\mathcal{P}$. Hence, the H_{s^2} ($H_{s^{*2}}$) belongs to the AIII class that is characterized by a Z invariant $v = N_s - N_{-s}$ ($v = N_{s^*} - N_{-s^*}$), which is equal to the number of MZM pairs on each wire end.

We next consider the compatibility between the different MZMs possessing different $\mathcal{S}$ eigenvalues. To do this, we introduce a coupling term $m|s_1\rangle\langle s_2|$, which satisfies the chiral symmetry, i.e. $\mathcal{S}m|s_1\rangle\langle s_2|\mathcal{S}^{-1} = -m|s_1\rangle\langle s_2| = ms_1s_2^*|s_1\rangle\langle s_2|$. Here m is a perturbation parameter, and $|s_1\rangle$ and $|s_2\rangle$ are the eigenstates of $\mathcal{S}$. Then we see that m can be nonzero only when $s_1s_2^* = -1$, which means that MZMs within one block having chiral eigenvalues s and $-s$ can couple to each other and be eliminated. However, MZMs from different blocks are noninterfering due to the protection of $\mathcal{S}$. Therefore, the topological classification of the whole BdG Hamiltonian is determined by the summation of the topology for each block. We summarize the topological classification of 1D gapped superconductors in Table 1 and analyse each case in the following.

(i) *$M_x\mathcal{T}$ and $C_{2z}\mathcal{T}$ cases.* These two cases are equivalent to the BDI class with $\mathcal{T}'^2 = 1$ and

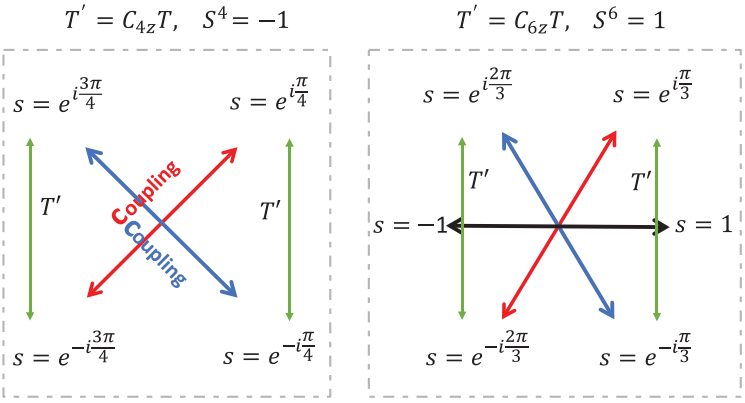

Figure 1. The eigenvalues of $\mathcal{S}$ and their transformations in the $C_{4z}\mathcal{T}$ and $C_{6z}\mathcal{T}$ cases. Complex conjugating partners s and s^* are related by the LMSs and always coexist. A perturbation term can be introduced to couple the chiral states with opposite eigenvalues, as illustrated by the red, blue and black double-head arrows.

$\mathcal{S}^2 = 1$. The chiral topological invariant $v = N_1 - N_{-1} \in Z$ is given by the winding number [5,26]

$$v = \frac{1}{2\pi}\int dk \mathrm{Tr}[W^\dagger(k)\partial_k W(k)] = \frac{1}{2\pi}\int dk \partial_k \theta(k). \quad (4)$$

Here $W(k)$ is a unitary matrix that diagonalizes the BdG Hamiltonian and $\theta(k)$ is the phase angle of $\mathrm{Det}[W(k)]$. The identity $\mathrm{Tr}[\ln(W)] = \ln(\mathrm{Det}[W])$ is used to derive the above equation. These results agree well with the conclusions reached in previous studies [34,36–38,40,41].

(ii) $C_{4z}\mathcal{T}$ *case*. The chiral symmetry satisfies $\mathcal{S}^4 = -1$ and has eigenvalues $\pm e^{\pm i\pi/4}$ (see Fig. 1). We can conclude that the topological invariants are given by $v = N_{e^{i\pi/4}} - N_{-e^{i\pi/4}}$ (or $N_{e^{-i\pi/4}} - N_{-e^{-i\pi/4}}$). The TSC phase is hence characterized by the helical topological invariant $v \in Z$, which means that the MZMs always appear in Kramers pairs. This is obviously different from the chiral Z invariant in the BDI class, in which the MZMs can arise one by one as Z increases. To distinguish the chiral Z and helical Z invariants, we use Z^c and Z^h in the following. The Z^h TSC phase of the $C_{4z}\mathcal{T}$-preserving wire can be understood from the following perspective. The BdG Hamiltonian can be block diagonalized into two sectors according to the eigenvalues $\pm i$ of $C_{2z} = (C_{4z}\mathcal{T})^2$ as $H_i(k) \oplus H_{-i}(k)$. Both $C_{4z}\mathcal{T}$ and $\mathcal{P}$ can map these two sectors to each other. However, their combination, i.e. the chiral symmetry $\mathcal{S}$, keeps each sector invariant. As a consequence, each sector belongs to the AIII class, whose Z^c topological invariant can be calculated by exploiting (4). Yielding to the $C_{4z}\mathcal{T}$ symmetry, the Z^c invariants of two sectors must be equal, which finally gives a Z^h invariant for the whole BdG Hamiltonian. That is, the topological invariant v is given by the winding number of each C_{2z} eigenvalue sector as defined in (4).

(iii) $C_{6z}\mathcal{T}$ *case*. We have $\mathcal{T}'^6 = 1$ and $\mathcal{S}^6 = 1$. As illustrated in Fig. 1, the chiral symmetry has eigenvalues $\pm e^{\pm i\pi/3}$, ± 1. The topology is characterized by $Z^h \oplus Z^c$ invariants that are given by $N_{e^{\pm i\pi/3}} - N_{-e^{\pm i\pi/3}}$ and $N_1 - N_{-1}$, respectively. Similar to the $C_{4z}\mathcal{T}$ case, the BdG Hamiltonian can be block diagonalized as $H = H_{e^{i2\pi/3}} \oplus H_{e^{-i2\pi/3}} \oplus H_1$ according to the eigenvalues $e^{\pm i2\pi/3}$, 1 of $C_{3z} = (C_{6z}\mathcal{T})^2$. The $H_{e^{i2\pi/3}}$ and $H_{e^{-i2\pi/3}}$ sectors both belong to the AIII class, forming a Z^h classification together, whereas the H_1 sector itself forms a Z^c classification (i.e. BDI class) with $\mathcal{P}$ and an effective $\mathcal{T}_{\mathrm{eff}} = (C_{6z}\mathcal{T})^3$. Therefore, the topology of the whole BdG Hamiltonian is classified by $Z^h \oplus Z^c$, whose topological invariants (v^h, v^c) are given by the winding numbers of the $H_{e^{i2\pi/3}}$ and H_1 sectors, respectively. As a consequence, in a 1D superconducting wire with the LMS $C_{6z}\mathcal{T}$, the helical and chiral MZMs can coexist. Such novel TSC phase stimulate further interests in the manipulation of such helical-chiral coexisting MZMs [42–44].

MODEL REALIZATION

To illustrate the TSC phase with the LMS $C_{4z}\mathcal{T}$, we construct a 1D antiferromagnetic chain along the z direction, as shown in Fig. 2(a), where each unit cell contains four subsites and each subsite is occupied by one spin polarized s orbital. We consider that the intra-cell coupling between the same spin states is much larger than the spin-orbit coupling, and thus the four orbitals are well split into two double-degenerate manifolds, as illustrated in Fig. 2(a). More details of the full model have been given in the online supplementary material. Here, to capture the topological phase of the model, we take the $|p_x, \uparrow\rangle$ and $|p_y, \downarrow\rangle$ subspaces to build an effective tight-binding model. Up to the nearest-neighbor hopping, it can be written as

$$H_{\mathrm{TB}}^{\mathrm{eff}} = \sum_l t c^\dagger_{l+1,p_x,\uparrow} c_{l,p_x,\uparrow} + t^* c^\dagger_{l+1,p_y,\downarrow} c_{l,p_y,\downarrow} + h.c. + \mu \sum_{l,\sigma} c^\dagger_{l\sigma} c_{l\sigma}, \quad (5)$$

where $t = |t|e^{i\alpha}$ is the complex hopping, μ is the chemical potential and σ acts on the orbital degree of freedom of the $|p_x, \uparrow\rangle$ and $|p_y, \downarrow\rangle$ states. The $C_{4z}\mathcal{T}$

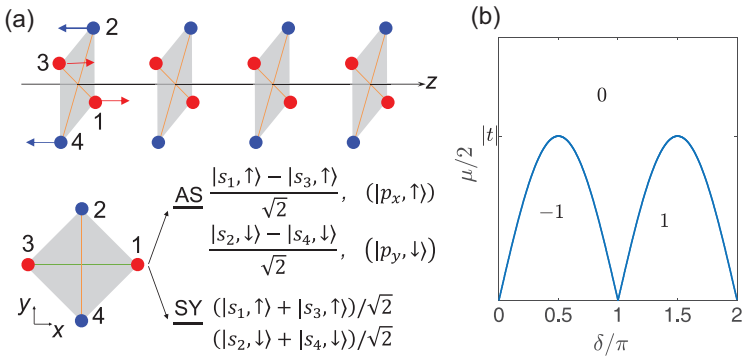

Figure 2. (a) A $C_{4z}\mathcal{T}$-preserving superconducting wire aligned along the z direction, in which the red and blue dots denote the spin up $(+z)$ and spin down $(-z)$ polarized s orbitals, respectively. The intra-cell coupling between the same spin orbitals is much larger than the spin-orbit coupling, which split the four states into one symmetric (SY) manifold and one antisymmetric (AS) manifold. Both manifolds are double degenerate. For simplicity, only the AS manifold is considered in our tight-binding model (5). (b) The topological phase diagram of (8) as the function of μ and δ, in which 0, ± 1 are the winding numbers, μ is the chemical potential and $\delta = \pi/2 + \phi - \alpha$ is the phase difference between the coefficients of τ_y and τ_z.

is given by $e^{i\pi/4\sigma_z}\sigma_y\mathcal{K}$. Note that the hopping terms between opposite spins are prohibited by the C_{2z} symmetry. The s-wave pairing Hamiltonian takes the form

$$H_\Delta = \sum_l \Delta c^\dagger_{l+1,p_x,\uparrow} c^\dagger_{l,p_y,\downarrow} + \Delta^* c^\dagger_{l+1,p_y,\downarrow} c^\dagger_{l,p_x,\uparrow} + h.c., \tag{6}$$

with $\Delta = |\Delta| e^{i\phi}$. The pairing terms between the same spin are also prohibited by the C_{2z} symmetry.

In the Nambu basis $(c_{k,p_x,\uparrow}, c^\dagger_{-k,p_y,\downarrow}, c_{k,p_y,\downarrow}, c^\dagger_{-k,p_x,\uparrow})^T$, $\mathcal{P}$ and $\mathcal{T}'$ are given by $\mathcal{P} = \sigma_x \otimes \tau_x\mathcal{K}$ and $\mathcal{T}' = e^{i\pi/4\sigma_z}\sigma_y \otimes I\mathcal{K}$, respectively, which give $\mathcal{S} = e^{-i\pi/4\sigma_z} \otimes \tau_x$. The BdG Hamiltonian anticommutes with $\mathcal{S}$ and takes a block-diagonal form as

$$H^{C_{4z}\mathcal{T}}_{\rm BdG}(k) = \begin{pmatrix} H_i(k) & \\ & H_{-i}(k) \end{pmatrix} \tag{7}$$

with

$$H_{\pm i}(k) = |t|\cos(k \pm \alpha)\tau_z - |\Delta|\sin(k \pm \phi)\tau_y + \frac{\mu}{2}\tau_z. \tag{8}$$

Then the spectrum is given by

$$E(k) = \pm\sqrt{\left[|t|\cos(k \pm \alpha) + \frac{\mu}{2}\right]^2 + |\Delta|^2 \sin^2(k \pm \phi)}. \tag{9}$$

Note that the two blocks in (7) are Kramers pairs related by the $C_{4z}\mathcal{T}$ symmetry and have the same winding number. A straightforward way to determine the topology is to calculate the winding number v using (4) for the upper or lower blocks. Here we provide a much simpler way to obtain v by analogizing the coefficients of the block Hamiltonians with elliptically polarized lights, whose electric field is described by $E_x = A_x\cos(kz - \omega t), E_y = A_y\cos(kz - \omega t + \delta)$. In the following we analyze the winding number of $H_i(k)$, where the coefficients of the Pauli matrices are $h_z - \mu/2 = |t|\cos(k + \alpha)$ and $h_y = |\Delta|\sin(k + \phi)$. When $|t||\sin\delta| > \mu/2$ $(<\mu/2)$, the parameter curve of $h_y(k)$ and $h_z(k)$ will (not) wind around the zero point $h_z = h_y = 0$ (we assume that $\mu > 0$ for simplicity), and the superconducting wire is in a topological nontrival (trivial) phase. Furthermore, when $\delta \in (0, \pi)$ $[\delta \in (-\pi, 0)]$, we have a left-handed (right-handed) parameter curve, and the topological phase is characterized by winding number $+1$ (-1). The phase diagram in the $\delta - \mu$ parameter space is plotted in Fig. 2(b). We point out that, when next-nearest-neighbor hopping and pairing are considered, the competition with nearest-neighbor hopping and pairing gives rise to the opportunity for TSC phase with higher winding numbers.

In the nontrivial TSC phase, the open quantum wire traps integer pairs of MZMs at its ends. By using $t = 1, \Delta = 1.3e^{i\pi/3}, \mu = 0.2$, we observe two pairs of MZMs in total on the open wire spectrum, as shown in Fig. 3(b), which is in contrast with the gapped bulk spectrum in Fig. 3(a). These MZMs can also be solved from the continuous low-energy model [45]. Here, we need only consider $H_i(k)$ since the other block in (7), as well as its zero energy solution, can be obtained by a $C_{4z}\mathcal{T}$ transformation. By assuming that the wire is placed on the $z > 0$ side, the low-energy massive Dirac Hamiltonian close to $k = \pi/2$ is given by

$$H_i = \begin{pmatrix} -i|t|\partial_z + \mu/2 & |\Delta|(-i\sin\delta + \cos\delta\partial_z) \\ |\Delta|(i\sin\delta - \cos\delta\partial_z) & i|t|\partial_z - \mu/2 \end{pmatrix}. \tag{10}$$

Its zero energy solution Ψ_1 and the $C_{4z}\mathcal{T}$-related partner $\Psi_2 = C_{4z}\mathcal{T}\Psi_1$ are given by

$$\Psi_1 = \begin{pmatrix} 1 \\ 1 \\ 0 \\ 0 \end{pmatrix} \exp\left[\int dz \frac{i|\Delta|\sin\delta - \mu/2}{|\Delta|\cos\delta - i|t|}\right], \tag{11}$$

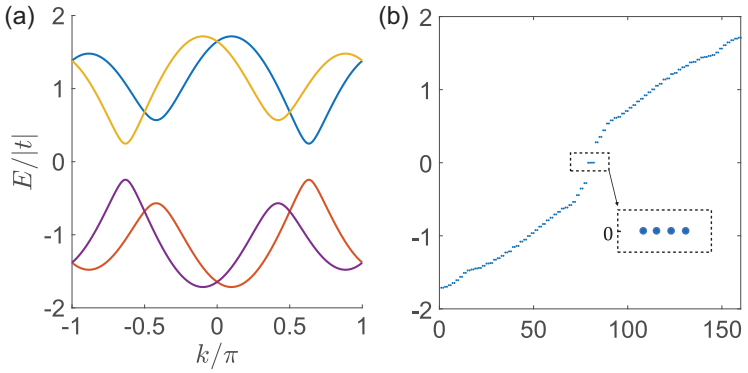

Figure 3. The bulk spectrum and MZMs in the $C_{4z}\mathcal{T}$-preserving TSC model. (a) The gapped bulk spectrum of the $C_{4z}\mathcal{T}$-preserving TSC phase with $t = 1$, $\Delta = 1.3e^{i\pi/3}$, $\mu = 0.2$. (b) The corresponding spectrum of (a) with an open boundary on both sides, in which four MZMs appear at zero energy.

$$\Psi_2 = \begin{pmatrix} 0 \\ 0 \\ 1 \\ 1 \end{pmatrix} \exp\left[\int dz \frac{-i|\Delta|\sin\delta - \mu/2}{|\Delta|\cos\delta + i|t|}\right]. \tag{12}$$

These two states are the eigenstates of the chiral symmetry $\mathcal{S}$ with eigenvalues $e^{\pm i\pi/4}$, respectively. Therefore, they are immune to perturbations preserving $\mathcal{S}$ (and $C_{4z}\mathcal{T}$). Their combinations give the $\mathcal{S}$ protected MZMs as $\gamma_1 = \Psi_1 + \Psi_2$ and $\gamma_2 = i(\Psi_1 - \Psi_2)$.

The $C_{4z}\mathcal{T}$-preserving BdG Hamiltonian can be easily generalized to a $C_{6z}\mathcal{T}$ invariant quantum wire. For this purpose, we assume that the chiral symmetry is expressed as $\mathcal{S} = (e^{-i\pi/3\tau_z} \otimes \tau_x) \oplus \tau_x$. The BdG Hamiltonian can then be written in three blocks $H_{\rm BdG}^{C_{6z}\mathcal{T}} = H_{e^{i2\pi/3}}(k) \oplus H_{e^{-i2\pi/3}}(k) \oplus H_1(k)$ with

$$\begin{aligned} H_{e^{\pm i2\pi/3}}(k) &= |t|\cos(k \pm \alpha)\tau_z \\ &\quad - |\Delta|\sin(k \pm \phi)\tau_y + \frac{\mu}{2}\tau_z, \\ H_1(k) &= |t'|\cos(k)\tau_z - |\Delta'|\sin(k)\tau_y \\ &\quad + \frac{\mu}{2}\tau_z. \end{aligned} \tag{13}$$

The first two blocks are Kramers pairs and take the same form as in (8), while the last block is transformed to itself under $C_{6z}\mathcal{T}$ or $\mathcal{P}$. For this BdG Hamiltonian, the topology is characterized by $Z^h \oplus Z^c$ numbers, which correspond to the number of helical and chiral MZMs, respectively. The topological phase diagram of the helical part Hamiltonian is the same as in Fig. 2(b). The chiral part is determined by the winding number of $H_1(k)$, which gives a nontrivial TSC phase when $|t'| > \mu/2$.

CONCLUSION

We have classified the TSC phases of quantum wires with LMSs. In the case of $M_x\mathcal{T}$ or $C_{2z}\mathcal{T}$, an equivalent BDI class TSC can be realized [37,38,40]. More importantly, we find two new types of TSC phases in the superconducting wire with $C_{4z}\mathcal{T}$ or $C_{6z}\mathcal{T}$, which are beyond the already known AZ classes and can be characterized by Z^h or $Z^h \oplus Z^c$ topological invariants, respectively. These results not only enrich the variety of the 1D TSC, but also provide luxuriant building blocks for the construction of new type 2D and 3D TSCs, by following the general method proposed in [46]. For example, one can couple the 1D TSCs in the y direction to construct a 2D TSC. The high symmetry lines $k_y = 0$ and $k_y = \pi$ in momentum space preserve the 1D LMS. With proper parameters, the $k_y = 0$ and $k_y = \pi$ lines can belong to distinct topological phases, and result in the gapless propagating Majorana edge states connecting the conducting bands and valence bands. The superconductivity and antiferromagnetism coexisting SmOFeAs [47,48] with a proper magnetic configuration satisfying $C_{4z}T$ symmetry is a possible material to study the 1D TSC phase on its high-symmetry lines.

SUPPLEMENTARY DATA

Supplementary data are available at *NSR* online.

ACKNOWLEDGEMENTS

The authors thank Chaoxing Liu for valuable discussions.

FUNDING

This work was supported by the National Key Research and Development Program of China (2018YFA0307000) and the National Natural Science Foundation of China (11874022).

AUTHOR CONTRIBUTIONS

Z.-D.S. and G.X. proposed the project. J.-Y.Z. carried out the topological classification and conceived the model. J.-Y.Z., Q.X., Z.-D.S. and G.X. analyzed the results. All authors contributed to the manuscript writing.

Conflict of interest statement. None declared.

REFERENCES

1. Kitaev AY. Unpaired Majorana fermions in quantum wires. *Phys Usp* 2001; **44**: 131–6.
2. Qi XL and Zhang SC. Topological insulators and superconductors. *Rev Mod Phys* 2011; **83**: 1057–110.
3. Sato M, Tanaka Y and Yada K *et al.* Topology of Andreev bound states with flat dispersion. *Phys Rev B* 2011; **83**: 224511.

4. Ando Y and Fu L. Topological crystalline insulators and topological superconductors: from concepts to materials. *Annu Rev Condens Matter Phys* 2015; **6**: 361–81.
5. Sato M and Ando Y. Topological superconductors: a review. *Rep Prog Phys* 2017; **80**: 076501.
6. Majorana E. Teoria simmetrica dell'elettrone e del positrone. *Nuovo Cim* 2008; **14**: 171.
7. Ivanov DA. Non-abelian statistics of half-quantum vortices in *p*-wave superconductors. *Phys Rev Lett* 2001; **86**: 268–71.
8. Kitaev AY. Fault-tolerant quantum computation by anyons. *Ann Phys* 2003; **303**: 2–30.
9. Nayak C, Simon SH and Stern A *et al.* Non-Abelian anyons and topological quantum computation. *Rev Mod Phys* 2008; **80**: 1083–159.
10. Sato M and Fujimoto S. Majorana fermions and topology in superconductors. *J Phys Soc Japan* 2016; **85**: 072001.
11. Fu L and Kane CL. Superconducting proximity effect and Majorana fermions at the surface of a topological insulator. *Phys Rev Lett* 2008; **100**: 096407.
12. Qi XL, Hughes TL and Zhang SC. Chiral topological superconductor from the quantum Hall state. *Phys Rev B* 2010; **82**: 184516.
13. Linder J, Tanaka Y and Yokoyama T *et al.* Unconventional superconductivity on a topological insulator. *Phys Rev Lett* 2010; **104**: 067001.
14. Wang MX, Liu C and Xu JP *et al.* The coexistence of superconductivity and topological order in the Bi_2Se_3 thin films. *Science* 2012; **336**: 52–5.
15. Xu JP, Liu C and Wang MX *et al.* Artificial topological superconductor by the proximity effect. *Phys Rev Lett* 2014; **112**: 217001.
16. Wang J, Zhou Q and Lian B *et al.* Chiral topological superconductor and half-integer conductance plateau from quantum anomalous Hall plateau transition. *Phys Rev B* 2015; **92**: 064520.
17. Fu L and Berg E. Odd-parity topological superconductors: theory and application to $Cu_xBi_2Se_3$. *Phys Rev Lett* 2010; **105**: 097001.
18. Hosur P, Ghaemi P and Mong R *et al.* Majorana modes at the ends of superconductor vortices in doped topological insulators. *Phys Rev Lett* 2011; **107**: 097001.
19. Tanaka Y, Sato M and Nagaosa N. Symmetry and topology in superconductors -odd-frequency pairing and edge states. *J Phys Soc Japan* 2012; **81**: 011013.
20. Fu L. Odd-parity topological superconductor with nematic order: application to $Cu_xBi_2Se_3$. *Phys Rev B* 2014; **90**: 100509.
21. Hosur P, Dai X and Fang Z *et al.* Time-reversal-invariant topological superconductivity in doped Weyl semimetals. *Phys Rev B* 2014; **90**: 045130.
22. Wang Z, Zhang P and Xu G *et al.* Topological nature of the $FeSe_{0.5}Te_{0.5}$ superconductor. *Phys Rev B* 2015; **92**: 115119.
23. Xu G, Lian B and Tang P *et al.* Topological superconductivity on the surface of Fe-based superconductors. *Phys Rev Lett* 2016; **117**: 047001.
24. Zhang P, Yaji K and Hashimoto T *et al.* Observation of topological superconductivity on the surface of an iron-based superconductor. *Science* 2018; **360**: 182–6.
25. Wang D, Kong L and Fan P *et al.* Evidence for Majorana bound states in an iron-based superconductor. *Science* 2018; **362**: 333–5.
26. Schnyder AP, Ryu S and Furusaki A *et al.* Classification of topological insulators and superconductors in three spatial dimensions. *Phys Rev B* 2008; **78**: 195125.
27. Ryu S, Schnyder AP and Furusaki A *et al.* Topological insulators and superconductors: tenfold way and dimensional hierarchy. *New J Phys* 2010; **12**: 065010.
28. Morimoto T and Furusaki A. Topological classification with additional symmetries from Clifford algebras. *Phys Rev B* 2013; **88**: 125129.
29. Benalcazar WA, Teo JCY and Hughes TL. Classification of two-dimensional topological crystalline superconductors and Majorana bound states at disclinations. *Phys Rev B* 2014; **89**: 224503.
30. Chiu CK, Teo JCY and Schnyder AP *et al.* Classification of topological quantum matter with symmetries. *Rev Mod Phys* 2016; **88**: 035005.
31. Cornfeld E and Chapman A. Classification of crystalline topological insulators and superconductors with point group symmetries. *Phys Rev B* 2019; **99**: 075105.
32. Zhang F, Kane CL and Mele EJ. Topological mirror superconductivity. *Phys Rev Lett* 2013; **111**: 056403.
33. Chiu CK, Yao H and Ryu S. Classification of topological insulators and superconductors in the presence of reflection symmetry. *Phys Rev B* 2013; **88**: 075142.
34. Shiozaki K and Sato M. Topology of crystalline insulators and superconductors. *Phys Rev B* 2014; **90**: 165114.
35. Fang C, Bernevig BA and Gilbert MJ. Topological crystalline superconductors with linearly and projectively represented C_n symmetry. arXiv: 1701.01944.
36. Mizushima T, Sato M and Machida K. Symmetry protected topological order and spin susceptibility in superfluid ^{3}He–*B*. *Phys Rev Lett* 2012; **109**: 165301.
37. Mizushima T and Sato M. Topological phases of quasi-one-dimensional fermionic atoms with a synthetic gauge field. *New J Phys* 2013; **15**: 075010.
38. Fang C, Gilbert MJ and Bernevig BA. New class of topological superconductors protected by magnetic group symmetries. *Phys Rev Lett* 2014; **112**: 106401.
39. Kopsky V and Litvin D (eds.). *International Tables for Crystallography: Subperiodic Groups*, Vol. E, 2nd edn. Dordrecht: Kluwer Academic Publishers, 2002.
40. Tewari S and Sau JD. Topological invariants for spin-orbit coupled superconductor nanowires. *Phys Rev Lett* 2012; **109**: 150408.
41. Samokhin KV. Superconductivity in quantum wires: a symmetry analysis. *Ann Phys* 2017; **385**: 563–83.
42. Tanaka Y, Yokoyama T and Nagaosa N. Manipulation of the Majorana fermion, Andreev reflection, and Josephson current on topological insulators. *Phys Rev Lett* 2009; **103**: 107002.
43. Alicea J, Oreg Y and Refael G *et al.* Non-abelian statistics and topological quantum information processing in 1D wire networks. *Nat Phys* 2011; **7**: 412–7.
44. Feng JJ, Huang Z and Wang Z *et al.* Hysteresis from nonlinear dynamics of Majorana modes in topological Josephson junctions. *Phys Rev B* 2018; **98**: 134515.
45. Bernevig BA and Hughes TL. *Topological Insulators and Topological Superconductors*. Princeton: Princeton University Press, 2013.
46. Song Z, Fang C and Qi Y. Real-space recipes for general topological crystalline states. arXiv: 1810.11013.
47. Yildirim T. Origin of the 150-K anomaly in LaFeAsO: competing antiferromagnetic interactions, frustration, and a structural phase transition. *Phys Rev Lett* 2008; **101**: 057010.
48. Mebrahtu A and Singh P. Coexistence of superconductivity and antiferromagnetism in SmAsO1-xFxFe. *World J Condens Matter Phys* 2015; **5**: 138–47.